# THE DETERMINATION OF NEAR-FIELD CORRECTION PARAMETERS FOR CIRCULARLY POLARIZED PROBES

A. C. Newell, M. H. Francis, D. P. Kremer
Electromagnetic Fields Division 723.05
Boulder, Colorado 80303 U.S.A.

In order to accurately determine the far-field of an antenna from near-field measurements the receiving pattern of the probe must be known so that probe correction can be performed. When the antenna to be tested is circularly polarized, the measurements are more accurate and efficient if circularly polarized probes are used. Further efficiency is obtained if one probe is dual polarized to allow for simultaneous measurements of both components. A procedure used by the National Bureau of Standards for determining the plane-wave receiving parameters of a dual-mode, circularly polarized probe is described herein. First, the on-axis gain of the probe is determined using the three antenna extrapolation technique. Second, the on-axis axial ratios and port-to-port comparison ratios are determined for both the probe and source antenna using a rotating linear horn. Far-field pattern measurements of both amplitude and phase are then made for both the main and cross components. In the computer processing of the data, the on-axis results are used to correct for the non-ideal source antenna polarization, scale the receiving coefficients, and correct for some measurement errors. The plane wave receiving parameters are determined at equally spaced intervals in k-space by interpolation of the corrected pattern data.

THE DETERMINATION OF NEAR-FIELD CORRECTION PARAMETERS
FOR CIRCULARLY POLARIZED PROBES

A. C. Newell, M. H. Francis, and D. P. Kremer
Electromagnetic Fields Division
National Bureau of Standards
Boulder, CO 80303

## I. Introduction

In order to accurately determine the far-field of an antenna from near-field measurements the receiving characteristics of the probe must be known so that probe correction can be performed [1,2,3,4]. We shall denote the complete, complex-vector, plane-wave spectrum, receiving characteristics of the probe by $\underline{s}'_{02}(\underline{K})$. A procedure used by the National Bureau of Standards for determining the receiving characteristics of a dual-mode, circularly polarized probe is described herein. To determine the receiving characteristics it is necessary to measure the amplitude and phase of the far-field pattern of the probe. In order to correctly determine the absolute magnitude of the receiving characteristics the on-axis gain is measured using the three antenna extrapolation technique [5]. The on-axis axial ratios of both the probe and source antenna are measured using a rotating linear horn so that the pattern measurements can be corrected for the non-ideal source polarization. Port-to-port comparison ratios are measured between the ports and between the main and cross components to provide the relative phase between the two ports and correct scaling for the cross component pattern. With the above measurements as input to the computer program the plane-wave receiving characteristics can be determined at equally spaced intervals in k-space by interpolation of the corrected pattern data. The computer program also performs a pattern integration to obtain the directivity. The following report describes the measurements performed and the data processing.

## II. Coordinate System Definition

The coordinate system of the probe must be clearly defined to allow precise and correct use of the measured data. Both the vector components of $\underline{s}'_{02}(\underline{K})$ and its directional dependence (specified by the values of $\underline{K}$) are defined with respect to the probe's coordinate system. The coordinate system must, therefore, be defined in a way that will ensure a permanent unambiguous reference and provide a convenient means of correctly aligning the probe when used in near-field measurements. For the probe under test, this was accomplished by scribed lines on the open end of the probe to define the x- and y-axes and by the normal to the aperture plane to define the direction of the z-axis.

The probe and its coordinates are shown schematically in figure 1. It is composed of a circular horn which has two ports, an R port (right circularly polarized), and an L port (left circularly polarized). The x and y coordinate axes are defined by two sets of scribed lines on the open end walls of the probe. The z-axis is defined as the normal to the aperture plane at the open end of the probe. It should be noted that the probe coordinates are defined with the positive z-axis <u>into</u> the probe, while in most applications the z-axis is defined as outgoing from the antenna. This particular definition is necessary when the probe is used as a near-field receiving antenna, where the coordinate systems of the antenna under test and the probe are parallel and in the same directions as shown in figure 2. In addition to the Cartesian coordinate system Oxyz, it is desirable to define spherical coordinates fixed to the antenna so that directions in space and vector components of the far field may be given in terms of two spherical angles. One choice for the definition of such a spherical coordinate system is shown in figure 3 for a general antenna. The z-axis is the polar axis and the angles $\theta$, $\phi$ and the unit vectors $\underline{e}_\theta$, $\underline{e}_\phi$ are defined as shown. In many cases, it is desirable to define the spherical angles such that the vector components are more constant in space in the region of the z-axis.

This can be done by choosing either the x- or y-axis as the polar axis; the choice of the y-axis gives rise to the coordinate system shown in figure 4. A given direction in space can, therefore, be defined by specifying either the components of the propagation vector $\underline{k}$ or any set of spherical angles, $\theta$, $\phi$; or A, E. Similarly, any vector which is transverse to the radial direction of the sphere can be expressed in terms of any of the sets of spherical components, $\underline{e}_\theta$, $\underline{e}_\phi$; or $\underline{e}_A$, $\underline{e}_E$. Transformation from one set of coordinates to the other may be accomplished by the equations,

$$\frac{k_x}{k} = \sin\theta \cos\phi = \sin A \cos E \tag{1}$$

$$\frac{k_y}{k} = \sin\theta \sin\phi = \sin E \tag{2}$$

$$\frac{k_z}{k} = \cos\theta = \cos A \cos E \,. \tag{3}$$

For a circularly polarized probe we are interested in the right and left components rather than the $\theta$ and $\phi$ components or the A and E components. The circular basis vectors are

$$\underline{e}_R = (\underline{e}_\theta + i\underline{e}_\phi)/\sqrt{2} \tag{4a}$$

$$\underline{e}_L = (\underline{e}_\theta - i\underline{e}_\phi)/\sqrt{2} \tag{4b}$$

for $\theta$, $\phi$ coordinates and

$$\underline{e}_R = (\underline{e}_A + i\underline{e}_E)/\sqrt{2} \tag{5a}$$

$$\underline{e}_L = (\underline{e}_A - i\underline{e}_E)/\sqrt{2} \tag{5b}$$

for A, E coordinates.

Then

$$\underline{v}_R = \underline{e}_R \, e^{i(kr - \omega t)} \tag{6a}$$

$$\underline{v}_L = \underline{e}_L \, e^{i(kr - \omega t)} \tag{6b}$$

represent right and left circularly-polarized plane waves traveling in the outward radial direction.

The receiving parameters $\underline{s}'_{02}$ $(\underline{K})$ are defined in terms of the antenna's response to incident plane waves. Therefore, $\underline{s}'_{02R}$ $(\underline{K})$ should couple only to an incident right circularly polarized plane wave and $\underline{s}'_{02L}$ $(\underline{K})$ only to an incident left circularly polarized wave. Thus

$$\underline{s}'_{02R}\ (\underline{K}) = (\underline{s}'_{02\theta} + i\underline{s}'_{02\phi})/\sqrt{2} \tag{7a}$$

$$\underline{s}'_{02L}\ (\underline{K}) = (\underline{s}'_{02\theta} - i\underline{s}'_{02\phi})/\sqrt{2} \tag{7b}$$

in $\theta$, $\phi$ coordinates.

## III. On-Axis Measurements

In the first step of the measurement process, a rotating linear horn was used to measure the on-axis polarization properties (axial ratio, tilt angle, and sense of polarization) of the probe and a dual-mode circularly polarized auxiliary source antenna. Accurate gain measurements were performed using a generalized three-antenna technique [5], since the probe's gain is also required for complete data processing.

From the axial ratio A, the tilt angle $\tau$, and the sense of polarization, the circular polarization ratio

$$\rho'_{sc}(0) \equiv \frac{s'_{02L}(0)}{s'_{02R}(0)} \tag{8}$$

is first obtained from the relations

$$|\rho'_{sc}(0)| = \frac{A(0) - 1}{A(0) + 1} \quad \text{if sense = Right}$$
$$= \frac{A(0) + 1}{A(0) - 1} \quad \text{if sense = Left} \tag{9}$$

$$\arg(\rho'_{sc}(0)) = 2\tau(0) \tag{10}$$

The sense of polarization is used to determine whether $|\rho'_{sc}(0)|$ is greater or less than unity since this information is not obtainable from the axial ratio or the tilt angle. During the polarization measurements, port-to-port measurements are also performed to measure the relative amplitude and phase between the two ports of each antenna. If a linearly polarized source horn is aligned with its field along the x-axis, and the receiver connected first to the R-port of the probe and then to the L-port, the ratio of these measured signals is

$$M_x = \frac{(1 - \Gamma_\ell \Gamma_{s''})\; s'_{02R}(0)\; (1 + \rho'_{sc}(0))}{(1 - \Gamma_\ell \Gamma_{s'})\; s''_{02L}(0)\; (1 + 1/\rho''_{sc}(0))} \tag{11}$$

where $\Gamma_\ell$, $\Gamma_{s'}$, $\Gamma_{s''}$ are respectively the reflection coefficients for the load, the R-port of the probe, and the L-port of the probe. In this and following equations, the single primed quantities refer to the R-port and the double primed quantities refer to the L-port. Since the reflection coefficients (obtained from measurements on the probes, source antenna, generator and load ports) and polarization ratios are known, the port-to-port ratio $s'_{02R}(0)/s''_{02L}(0)$ may be found.

The on-axis magnitude for the main component of the R-port is obtained from the relationship (see Eq. 1.6-19 Ref. 1)

$$s'_{02R}(0) = \left[ \frac{(1 - |\Gamma_{s'}|^2)\, Y_0\, G_{s'}(0)}{4\pi\, k^2\, (1 - |\rho'_{sc}(0)|^2)\, \eta_0} \right]^{1/2} \qquad (12)$$

where $G_{s'}(0)$ is the measured gain for the R-port in the on-axis direction, $\Gamma_{s'}$ is the reflection coefficient of the R-port, and $Y_0$ and $\eta_0$ are admittance factors which, for this purpose, may be taken as being equal, $\eta_0 = Y_0$. The phase of $s'_{02R}(0)$ may be chosen arbitrarily, and the magnitude and phase of the cross component are then obtained from the polarization ratio,

$$s'_{02L}(0) = \rho'_{sc}(0)\; s'_{02R}(0) \; . \qquad (13)$$

For the L-port, similar data are used to obtain its on-axis components denoted $s''_{02R}(0)$ and $s''_{02L}(0)$. In this case, the L-component is the major component. The gain for this port is used to set the magnitude of $s''_{02L}(0)$, the port-to-port comparison data are used to set the phase of $s''_{02L}(0)$ relative to $s'_{02R}(0)$, and the magnitude and phase of $s''_{02R}$ is set relative to $s''_{02L}(0)$ by

$$s''_{02R}(0) = \frac{s''_{02L}(0)}{\rho''_{sc}(0)} \; . \qquad (14)$$

## IV. Relative Pattern Measurements

The final step in the measurement process is the measurement of both amplitude and phase of the relative receiving pattern of the probe for two nominally orthogonal incident fields. To do this, the probe is placed on a model mount rotator on a far-field range, as shown in figure 5, with a CP auxiliary antenna being used as the source antenna. For these measurements, both the probe and source antennas are aligned with their y-axes in the vertical direction for $\phi = 0$ of the rotator and with their z-axes directed along the line between them for $\theta = 0$. The probe is then rotated about its z-axis by the angle $\phi$ and about a vertical axis (the azimuth axis of the rotator) by the angle $\theta$. The directions of rotation in $\theta$ and in $\phi$ are such that for positive $\theta < \pi/2$ and positive $\phi < \pi/2$, the plane-wave incident upon the probe from the source antenna is one with positive values of all components of the propagation vector, $k_x$, $k_y$, $k_z > 0$ as shown in figure 6. The proper sense of rotation will ensure the correct attribution of the data to directions specified by $(\theta, \phi)$ or $(k_x, k_y)$ and, therefore, allow the use of the transformation eqs (1) - (3). It should be noted that since the z-axis is defined as directed into the probe and measurements are required for positive values of $k_z$, the appropriate half of the measurement sphere is behind the probe. As viewed from the front of the probe, it may at first appear that the angles are not conventionally defined, or that left-handed coordinates are being used, but the apparent conflict is due to the different point of view. For these pattern measurements, $\theta$ is varied continuously from -100° to +100° and $\phi$ is stepped from zero to -360°. The negative values of $\phi$ result from the inward directed z-axis of the probe and the "normal" $\phi$-rotation of the rotator mount being used. As a result of the $\phi$ variations over 360° along with the $\theta$ variation over ±100°, two measurements are obtained for each direction relative to the probe. These two measurements are averaged to reduce the effect of scattering within the room. Figure 7 shows a sample of data before averaging and figure 8 is after averaging.

Four sets of pattern data are obtained corresponding to the combinations of source polarization and probe output port. If we denote the on-axis transmitting coefficients of the R-port on the source antenna as $h_R$ and $h_L$ and the receiving coefficients of the R-port of the probe as $s'_R$ and $s'_L$, then the first set of relative pattern data for the right circular source and right circular probe port is

$$\beta_1(\theta,\phi) = \frac{B_{RR}(\theta,\phi)}{B_{RR}(0,0)} = \frac{h_R\ s'_R(\theta,\phi) + h_L\ s'_L(\theta,\phi)}{h_R\ s_R(0,0) + h_L\ s'_L(0,0)} \tag{15}$$

$$= \frac{s'_R(\theta,\phi) + p_{hc}\ s'_L(\theta,\phi)}{s'_R(0,0) + p_{hc}\ s'_L(0,0)}\ .$$

The input signal is next connected to the left circular port of the source, whose on-axis transmitting coefficients are denoted $u_R$ and $u_L$. These pattern data as well as the additional two sets for the probe's L-port are also measured relative to the R-component maximum so that the probe's receiving coefficients for both ports and components will be measured with respect to the same phase reference. In a similar way, data are obtained for the left circular port of the probe using both ports of the source. Denoting the probe coefficients for the L-port as $s''_R$ and $s''_L$ the four measurement equations are

$$\beta_1(\theta,\phi) = \left[\frac{1}{s'_R(0,0) + p_{hc}\ s'_L(0,0)}\right]\left(s'_R(\theta,\phi) + p_{hc}\ s'_L(\theta,\phi)\right) \qquad (16)$$

$$\beta_2(\theta,\phi) = \frac{(1 - \Gamma_g \Gamma_h)\ u_L}{(1 - \Gamma_g \Gamma_u)\ h_R\ \left(s'_R(0,0) + p_{hc}\ s'_L(0,0)\right)} \left(s'_R(\theta,\phi)/p_{uc} + s'_L(\theta,\phi)\right) \qquad (17)$$

$$\beta_3(\theta,\phi) = \left[\frac{(1 - \Gamma_g \Gamma_h)\ (1 - \Gamma_\ell \Gamma_{s''})\ u_L}{(1 - \Gamma_g \Gamma_u)\ (1 - \Gamma_\ell \Gamma_{s'})\ h_R\ \left(s'_R(0,0) + p_{hc}\ s'_L(0,0)\right)}\right] \left(s''_R(\theta,\phi)/p_{uc} + s''_L(\theta,\phi)\right) \qquad (18)$$

$$\beta_4(\theta,\phi) = \left[\frac{(1 - \Gamma_\ell \Gamma_{s''})}{(1 - \Gamma_\ell \Gamma_{s'})\ \left(s'_R(0,0) + p_{hc}\ s'_L(0,0)\right)}\right] \left(s''_R(\theta,\phi) + p_{hc}\ s''_L(\theta,\phi)\right) \qquad (19)$$

where $\Gamma_g$, $\Gamma_\ell$, $\Gamma_h$, $\Gamma_u$, $\Gamma_{s'}$, $\Gamma_{s''}$ are respectively the reflection coefficients of the generator, load, source right port, source left port, probe right port, and probe left port. The p's are the circular polarization ratio for the source

$$p_{hc} = \frac{h_L}{h_R} \ll 1 \tag{20}$$

$$p_{uc} = \frac{u_L}{u_R} \gg 1 \ . \tag{21}$$

In summary, the data available for the computer processing are the following:

(1) the on-axis gain and polarization of both ports of the probe and both ports of the source,
(2) the reflection coefficients for the source, probe, generator, and load,
(3) the ratio $s_L''(0)/s_R'(0)$, and
(4) the relative pattern data, $\beta_1(\theta,\phi)$, $\beta_2(\theta,\phi)$, $\beta_3(\theta,\phi)$, $\beta_4(\theta,\phi)$.

## V. Computer Processing

It can be shown that for $\theta = 0$, when the probe is directed toward the source horn, the $\phi$-dependence of each component of the measured data is prescribed in terms of the previously measured polarization parameters by the equations,

$$\beta_1(0,\phi) = \frac{\cos(\psi + \phi) + i\, R'\sin(\psi + \phi)}{\cos(\psi) + i\, R'\sin(\psi)} \tag{22}$$

where $\psi$ is the sum of the tilt angles of the two antennas

$$\psi = \tau_h + \tau_s' \ , \tag{23}$$

and R is obtained from the circular polarization ratios by the relation

$$R' = \frac{p_{hc}(0)\ \rho_{sc}'(0) \ - 1}{p_{hc}(0)\ \rho_{sc}'(0) \ + 1} \tag{24}$$

In principle the axial ratio and tilt angle of the source and probe as determined by the on-axis measurements should be used in the data processing to do source correction and specify the $\phi$-dependence for $\theta = 0$ (see eqs (22)-(24)). However, in some cases it is found that the cross component pattern measurements were not always consistent with these values. It was determined during the on-axis measurements that the axial ratio and tilt angle of one port can critically depend upon the impedance of the termination connected to the unused port and the impedance of the transmission line connected to the port being measured. These problems affect the cross polarized pattern measurements and are most pronounced when one of the probes had a very low axial ratio. The effect is observed by comparing the $\phi$-pattern for $\theta = 0$ , $\beta(0,\phi)$, predicted by the on-axis measurements to that obtained during pattern measurements. From eqs. (22)-(24) it is apparent that if the axial ratio and tilt angle of the probe and source are known, the minimum value of $\beta(0,\phi)$ and the location of the minimum are determined. In those cases where the predicted and observed values significantly differed, the axial ratio and tilt angle of the source and/or probe were adjusted slightly to be consistent with the pattern data.

All of the pattern measurements are relative values and the desired end results are absolute, correctly scaled values for the receiving components. This correct scaling of equations is obtained from the absolute, on-axis gain and polarization measurements. All of the terms in the factors within the square brackets of eqs (16)-(19) are known from the on-axis measurements (see eqns. 12-14). Evaluating those factors and dividing the corresponding pattern data by them gives us the four equations on an absolute scale. The process referred to as source correction then gives the results

$$s_R'(\theta,\phi) = \frac{\beta_1'(\theta,\phi) - p_{hc}(0)\,\beta_2'(\theta,\phi)}{1 - p_{hc}(0)/p_{uc}(0)} \tag{25}$$

$$s_L'(\theta,\phi) = \frac{\beta_2'(\theta,\phi) - \beta_1'(\theta,\phi)/p_{uc}(0)}{1 - p_{hc}(0)/p_{uc}(0)} \tag{26}$$

$$s_L''(\theta,\phi) = \frac{\beta_3'(\theta,\phi) - \beta_4'(\theta,\phi)/p_{uc}(0)}{1 - p_{hc}(0)/p_{uc}(0)} \tag{27}$$

$$s_R''(\theta,\phi) = \frac{\beta_4'(\theta,\phi) - p_{hc}(0)\ \beta_3'(\theta,\phi)}{1 - p_{hc}(0)/p_{uc}(0)} \tag{28}$$

where the $\beta'$'s are the results of the correct scaling of the $\beta$'s using the on-axis values of gain and polarization.

The results of eqs (25)-(28) are the desired probe-receiving parameters. One final correction is made on the probe coefficients to obtain a more convenient phase variation as a function of direction. From equations 10 and 13 it is apparent that the phase of the receiving components is related to the tilt angle. A value for the tilt angle specifies the location of the major axis of the polarization ellipse with respect to some coordinate system fixed to the antenna under test. To define the coordinate system, lines are first scribed on the probe to fix the x and y axes. For the on-axis direction where both $\theta$ and $\phi$ are zero, the tilt angle is measured with respect to the x-axis going toward the y-axis. For other directions the tilt angle will depend on the spherical coordinates used for the pattern measurements. For example, if an A-E coordinate system is used (see figure 9) the tilt angle is measured with respect to lines of constant E. For the $\theta$-$\phi$ coordinate system, used in the present measurements, the tilt angle is measured with respect to lines of constant $\phi$. Both of these are "correct" for the given coordinate system. However, in the second case the tilt angle varies with $\phi$ since the lines of constant $\phi$ vary more rapidly with respect to the antenna than the lines of constant E in the A-E coordinate system. Because of this and also because the tilt angle is discontinuous at $\theta = 0$, $\phi = 0$, the $\theta$-$\phi$ coordinates, although correct, are not very convenient. It is, therefore desirable to transfer the tilt angle measurements to another coordinate system. It is possible to transfer to the A-E coordinates but the easiest one is similar to the θ-ϕ coordinates but with a rotation of the tilt angle by the angle ϕ (see figure 10). For this coordinate system the new tilt angle, $\tau'$, in terms of the tilt angle, $\tau$, of the θ-ϕ coordinate system is

$$\tau' = \tau + \phi \tag{29}$$

This value of the tilt angle, $\tau'$, is equivalent to the tilt angle which would be measured if the source antenna had been rotated by ϕ in synchronization with the probe under test. This is often done with model mount measurement systems.

This last coordinate system implies that for $\theta = 0$ the probe corrected patterns should be constant in amplitude and phase as a function of ϕ. This dependence is enforced upon the source corrected data by requiring

$$s_R'(0,\phi) = s_R'(0,0) \tag{30}$$

$$s_L'(0,\phi) = \rho_{sc}'(0)\; s_R'(0,0) \tag{31}$$

$$s_L''(0,\phi) = s_L''(0,0) \tag{32}$$

$$s_R''(0,\phi) = \frac{s_L''(0,0)}{\rho_{sc}''(0)} \tag{33}$$

At this point the results are still given on a measurement grid which is equally spaced in θ and in ϕ; in the programs which use these parameters, they are required on a grid equally spaced in $k_x$ and $k_y$. The next step in the processing is to interpolate the data to the required increments. A four-point linear interpolation is used utilizing the four measurement points adjacent to the required values of $k_x$ and $k_y$ as shown in figure 11. Since the probe pattern is generally quite smooth and varies slowly, the linear interpolation is quite accurate. At the conclusion of the interpolation process, the computer program provides the desired probe-receiving parameters $s_R'(k_x, k_y)$, $s_L'(k_x, k_y)$, $s_L''(k_x, k_y)$ and $s_R''(k_x, k_y)$. These parameters are used in the probe-correction equations and programs. This means that the parameters describe the properties of the probe when it is aligned on the near-field scanner with its x-, y-, and z-axes parallel to those of the antenna under test. In general, near-field measurements are required for two independent probes. In this case, the second probe is the other port of the CP probe.

During the data processing pattern integration is performed so as to obtain the on-axis directivity. Since the difference between the on-axis gain and on-axis directivity is due to ohmic losses which are usually small, this serves as a check on the gain measurements.

## VI. Results

The major output of these tests are magnetic tapes containing both the measured data and samples of the final probe parameters obtained from the computer processing. Associated with the tape outputs are graphical displays of the results which are useful in understanding the general character of the probe parameters.

## VII. Estimates of Error

An example of the estimates of error for the on-axis measurements are shown in the tables below. In each case, the final error estimates are the result of a quadrature sum (root sum square) of the individual error components. Each error component is either a worst case or a 3-$\sigma$ value, and the errors are independent and uncorrelated. The confidence level for the resulting combination is therefore equivalent to that associated with $3\sigma$.

In this example SMA connectors were used and the specific antenna had a specific associated isolation. With waveguide flanges or improved precision connectors and improved isolation between the two ports it is expected that the errors would be less than this example.

Table 1. Errors in gain measurement

| Source of Error | Resultant Error in Gain (dB) |
|---|---|
| System Drift and Receiver Nonlinearity | 0.05 |
| Attenuator Calibration | 0.04 |
| Impedance Mismatch | <0.01 |
| Antenna Alignment | 0.05 |
| Distance Nonlinearity | 0.02 |
| Connector Variability | 0.14 |
| Residual Multipath | 0.03 |
| Random Errors | 0.03 |
| Quadrature Sum | ±0.17 |

Table 2. Errors in axial ratio measurements

| | Axial ratio errors (dB) for axial ratios of (dB) | | | | |
|---|---|---|---|---|---|
| Source of error | 0.05 | 0.10 | 0.20 | 0.30 | 0.40 |
| Antenna alignment and multipath | 0.03 | 0.02 | 0.02 | 0.02 | 0.02 |
| Connector variability | 0.08 | 0.05 | 0.05 | 0.04 | 0.04 |
| RSS | ±0.09 | ±0.05 | ±0.05 | ±0.05 | ±0.05 |

Table 3. Errors in tilt angle measurements

| Source of error | Tilt angle errors (degrees) for axial ratios of (dB) 0.05 | 0.10 | 0.20 | 0.30 | 0.40 |
|---|---|---|---|---|---|
| Antenna alignment and multipath | 30 | 10 | 6.5 | 3.5 | 3.5 |
| Connector variability | 40 | 32 | 10 | 10 | 10 |
| RSS | ±50 | ±34 | ±12 | ±11 | ±11 |

A number of tests were made to determine the magnitude and effect of various sources of error which would perturb the pattern measurements. These included tests for probe alignment, reflections within the test range, near-zone effects, receiver linearity, rotator alignment and accuracy, and leakage signals. The probe was first aligned mechanically and then checked by electrical means. The electrical tests consisted of measuring a pair of pattern cuts for $\phi = 0°$ and $\phi = -180°$ or for $\phi = -90°$ and $\phi = -270°$. If the θ- and ϕ-axes of the mount did not interesect, or if the z-axis of the probe was not coincident with the ϕ-axis of the rotator, anomalies would occur in the phase patterns. In the test performed, the phase patterns agreed to within 4° for both $\phi = 0$ and $\phi = -90°$ patterns over the range of θ from -90° to +90°. Range reflection tests were carried out by essentially conducting field probes in the x-, y-, and z-directions. These indicated that reflections from floor, ceiling, side walls, and multiple reflections between source and probe could cause an amplitude error of 0.1 dB maximum in the main component for regions close to $\theta = 0$. This is equivalent to a reflectivity level of -45 dB. When the probe was rotated to the region of $\theta = 90°$, reflections from the back wall had the predominant effect. These were found to cause a variation in the pattern of 0.25 dB peak-to-peak for the main component, and 3 dB peak-to-peak for the cross component. As described in section IV the pattern data is obtained twice at each measurement point and averaged. This averaging will tend to reduce the effects of room reflections. Patterns were made at a sufficient distance from the

Table 4. Main-component pattern errors

| Source of error | Amplitude errors (dB) for amplitude levels (dB) | | | Phase errors (deg.) for amplitude levels (dB) | | |
|---|---|---|---|---|---|---|
| | -5 | -15 | -30 | -5 | -15 | -30 |
| Room reflections | 0.09 | 0.27 | 1.57 | 0.8 | 1.81 | 11 |
| Probe alignment | 0.05 | 0.10 | 0.20 | 1 | 2 | 3 |
| Receiver nonlinearity | 0.01 | 0.03 | 0.05 | -- | -- | -- |
| Receiver phase error | -- | -- | -- | 1 | 2 | 3 |
| Near-zone effects | 0.05 | 0.15 | 0.30 | 0.3 | 1 | 2 |
| Rotator error | 0.02 | 0.05 | 0.08 | -- | -- | -- |
| RSS | ±0.12 | ±0.33 | ±1.61 | ±1.6 | ±3.5 | ±12 |

source antenna that the amplitude taper across the major dimension of the probe was less than 0.2 dB and, therefore, introduced a very small error in the patterns. Receiver linearity was checked with a calibrated rotary vane attenuator and adjustments made to the measured data to correct for most of the error. Leakage tests indicated that all sources of interfering signals were below the -55 dB level relative to the peak of the main component. The results of these tests are summarized in table 4. The amplitude levels of -5, -15, and -30 dB used in the table are with respect to the main component maximum.

In conclusion then, the procedure described above can be used to determine the receiving parameters of a dual-mode circularly polarized probe.

## VIII. References


[1] Kerns, D. M. Plane-wave scattering-matrix theory of antennas and antenna-antenna interaction. Nat. Bur. Stand. (U.S.) NBSIR 78-890; 1978.

[2] Newell, A. C.; Crawford M. L. Planar near-field measurements on high performance array antennas. Nat. Bur. Stand. (U.S.) NBSIR 74-380; 1974.

[3] Newell, A. C. Upper bound errors in far-field antenna parameters determined from planar near-field measurements part 2: Analysis and computer simulation. Nat. Bur. Stand. (U.S.) report (unpublished); 1975 July.

[4] Joy, E. B. and Paris, D. T. Spatial sampling and filtering in near-field measurements. IEE Trans. Antennas and Prop. AP-20: 253-261; 1972 May.

[5] Newell, A. C.; Baird, R. C.; Wacker, P. F. Accurate measurement of antenna gain and polarization at reduced distances by an extrapolation technique. IEEE Trans. Antennas Prop. AP-21: 418-31; 1973.

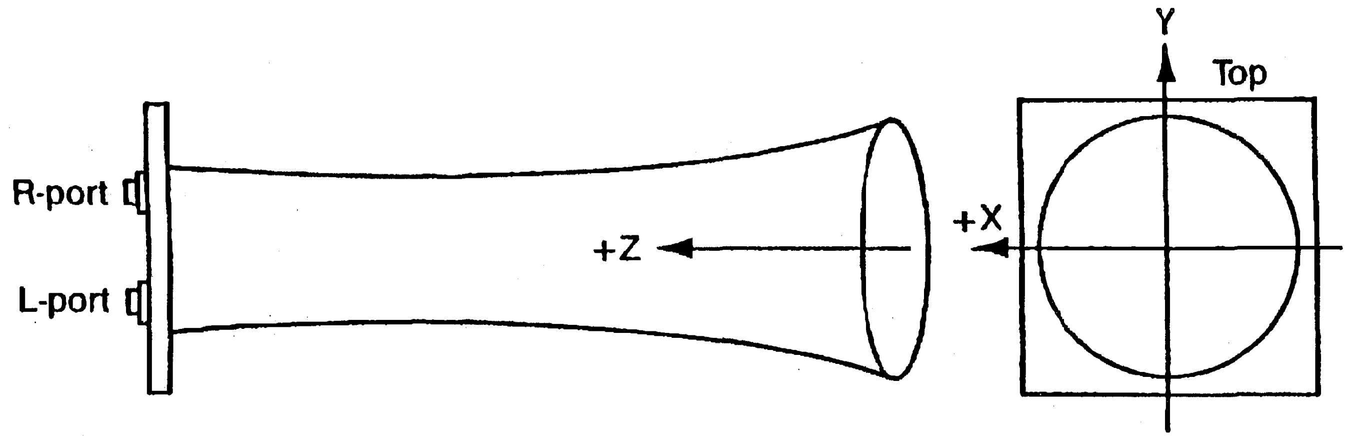


Figure 1. Schematic of circular probe showing the definition of the coordinate axes.

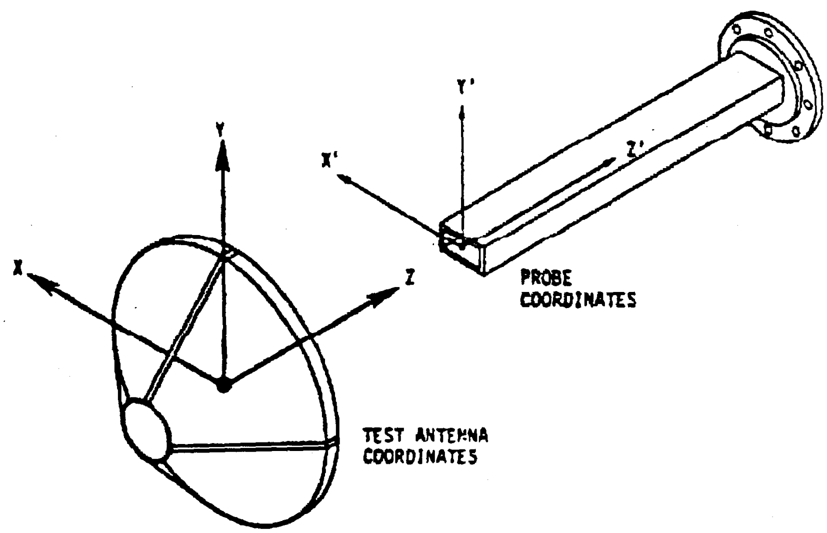


Figure 2. Relative orientation of the probe and test antenna coordinates for planar near-field measurements.

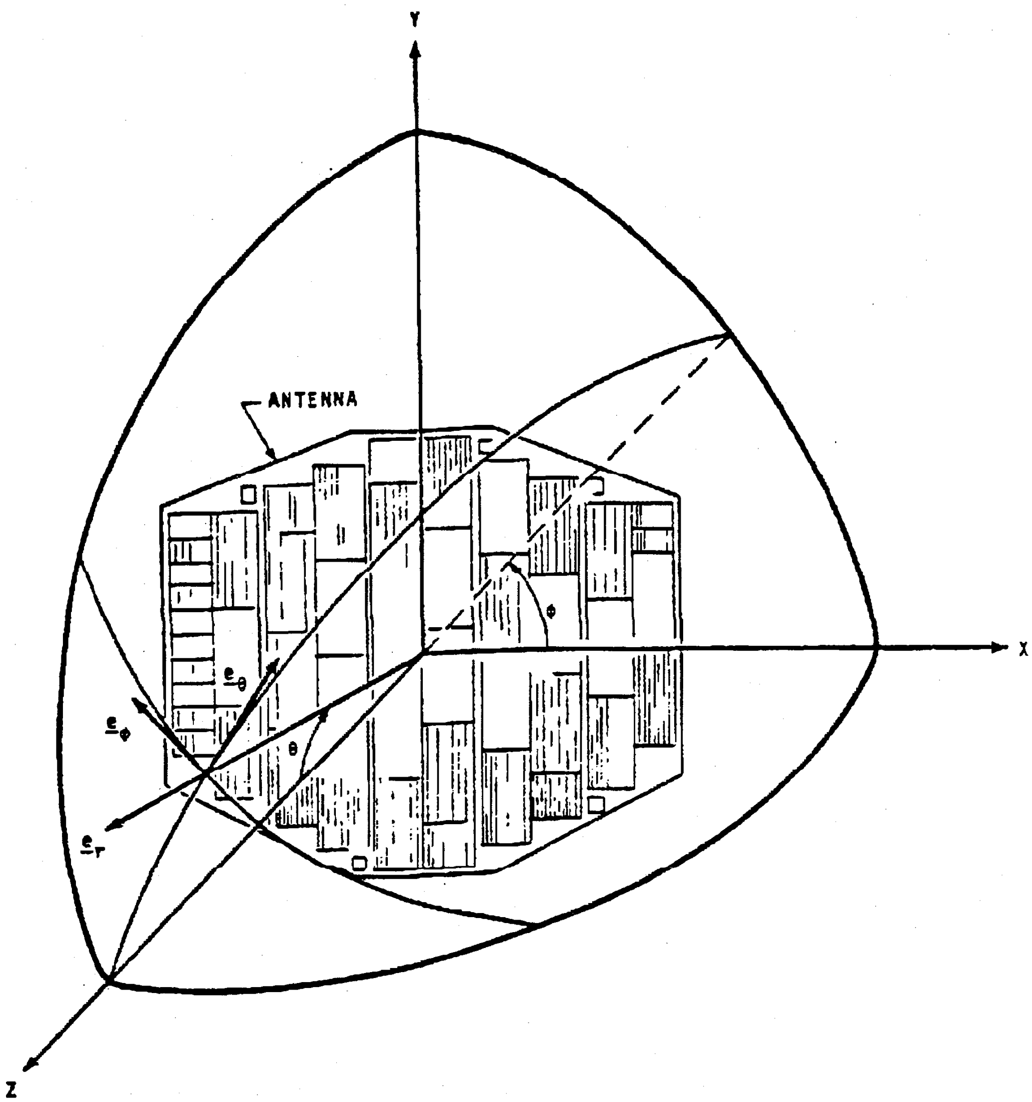


Figure 3. Antenna coordinate system using θ and φ spherical angles with z as the polar axis.

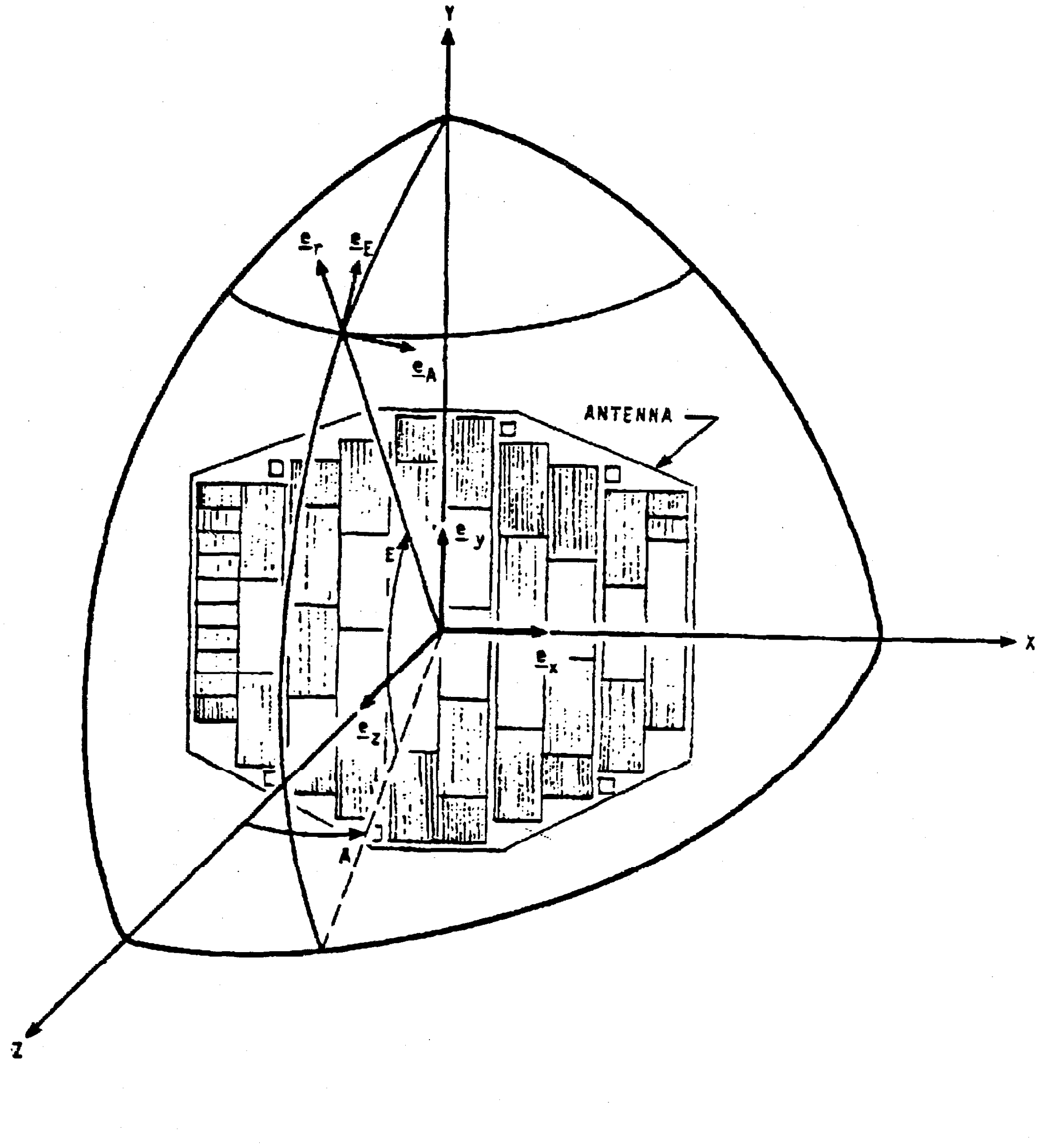


Figure 4. Antenna coordinate system using A and E spherical angles with Y as the polar axis.

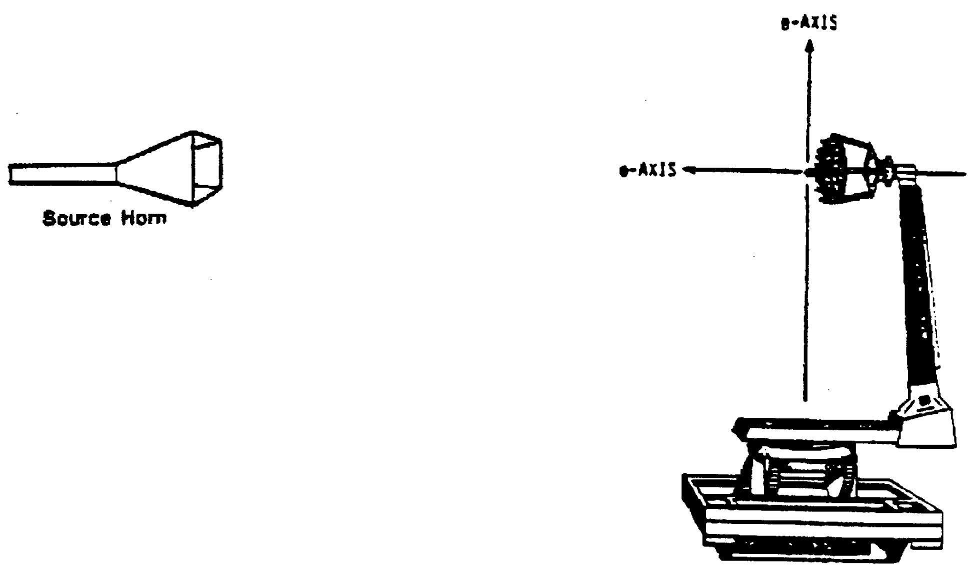


Figure 5. Probe on model tower rotator for pattern measurements.

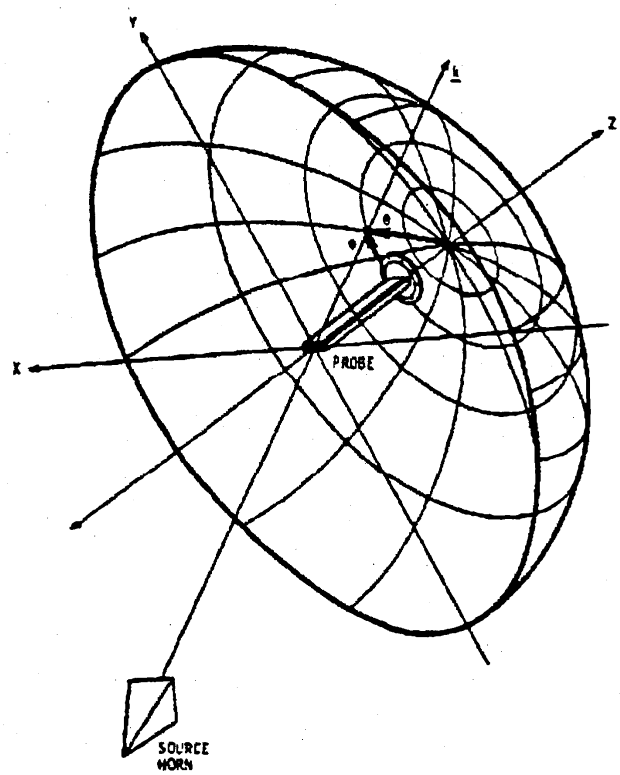


Figure 6. Probe and its spherical coordinate system showing the direction ($\underline{K}$) of an incident plane wave from the source horn with $k_x$, $k_y$, and $k_z$ all positive. Correct values of $k_x$, $k_y$, and $k_z$ are obtained by positive rotation of the probe in $\theta$ and $\phi$ of less than $90^0$ as shown.

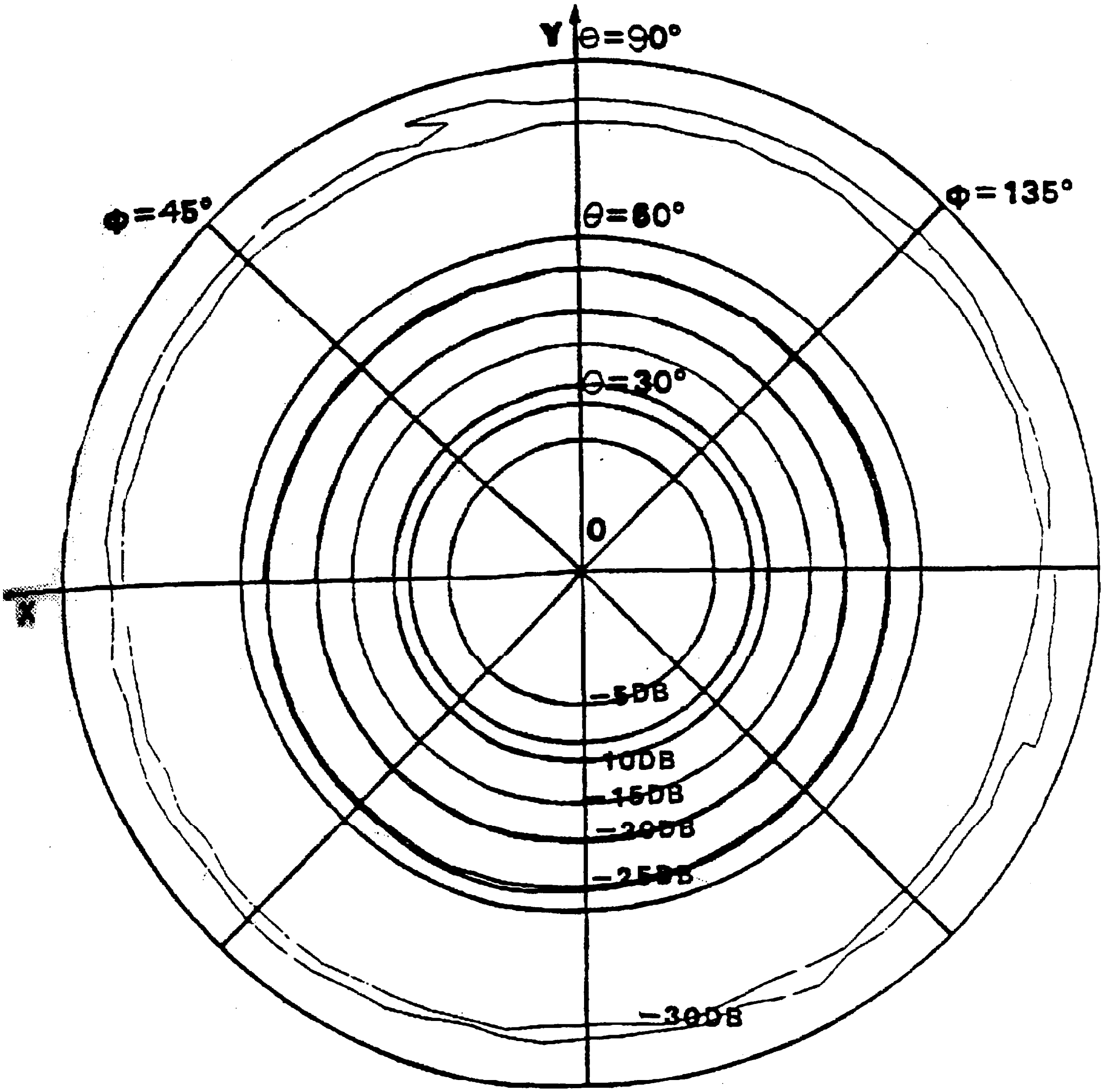


Figure 7. Contour plot of the amplitude for a typical pattern measurement before averaging, amplitudes relative to the peak, 5dB contours.

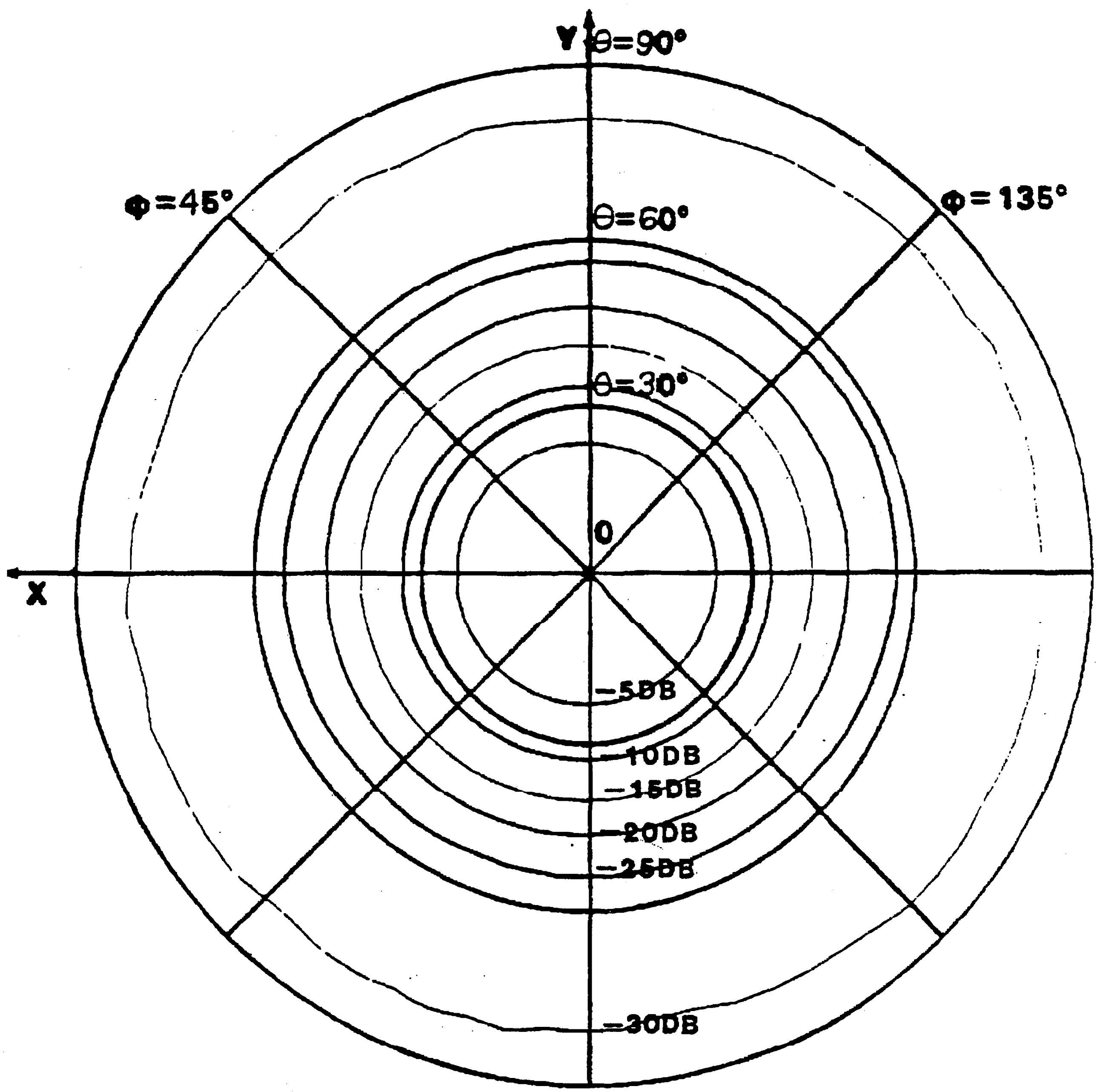


Figure 8. Contour plot of the amplitude for a typical pattern measurement after averaging, amplitudes relative to the peak, 5db contours.

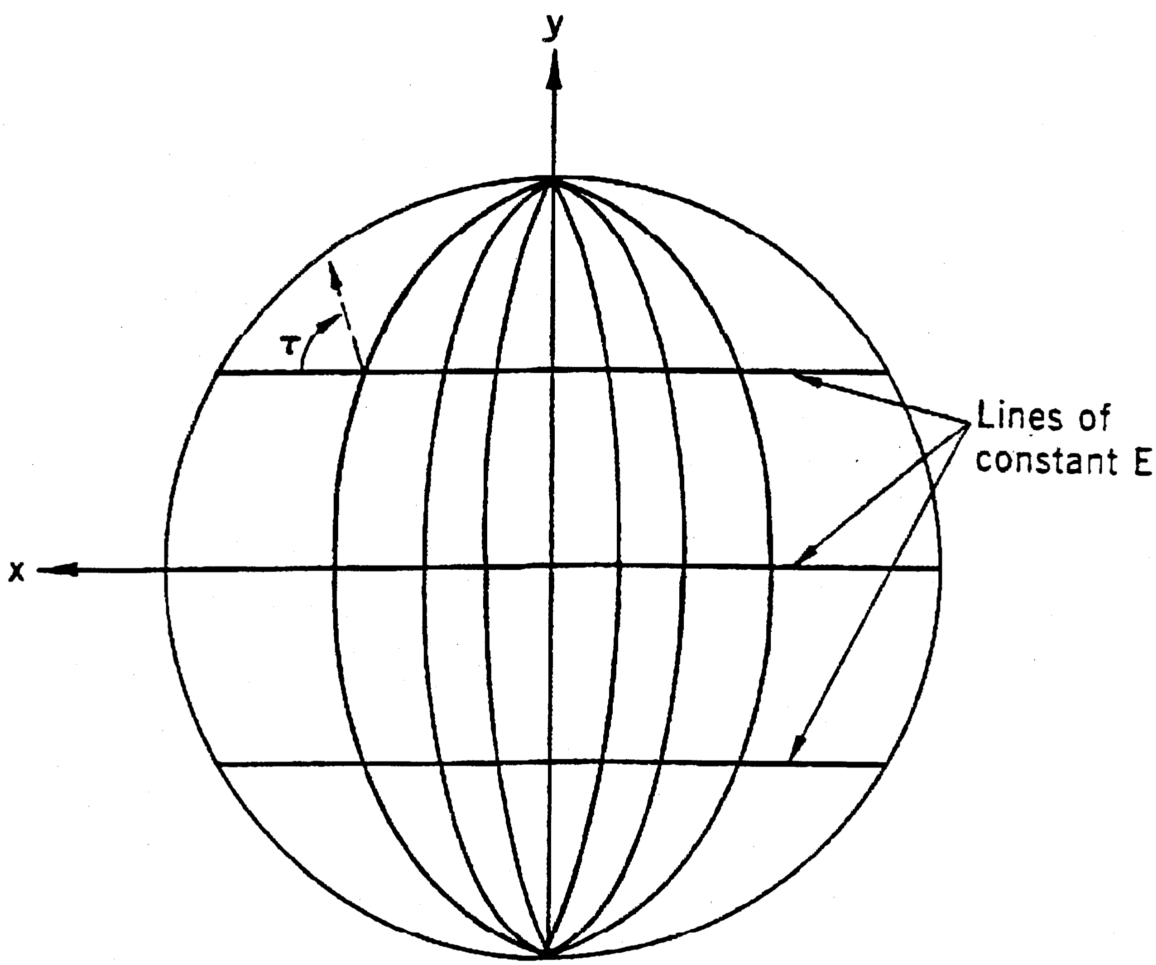


Figure 9. Schematic showing how the tilt angle, $\tau$, is measured in the A-E coordinate system.

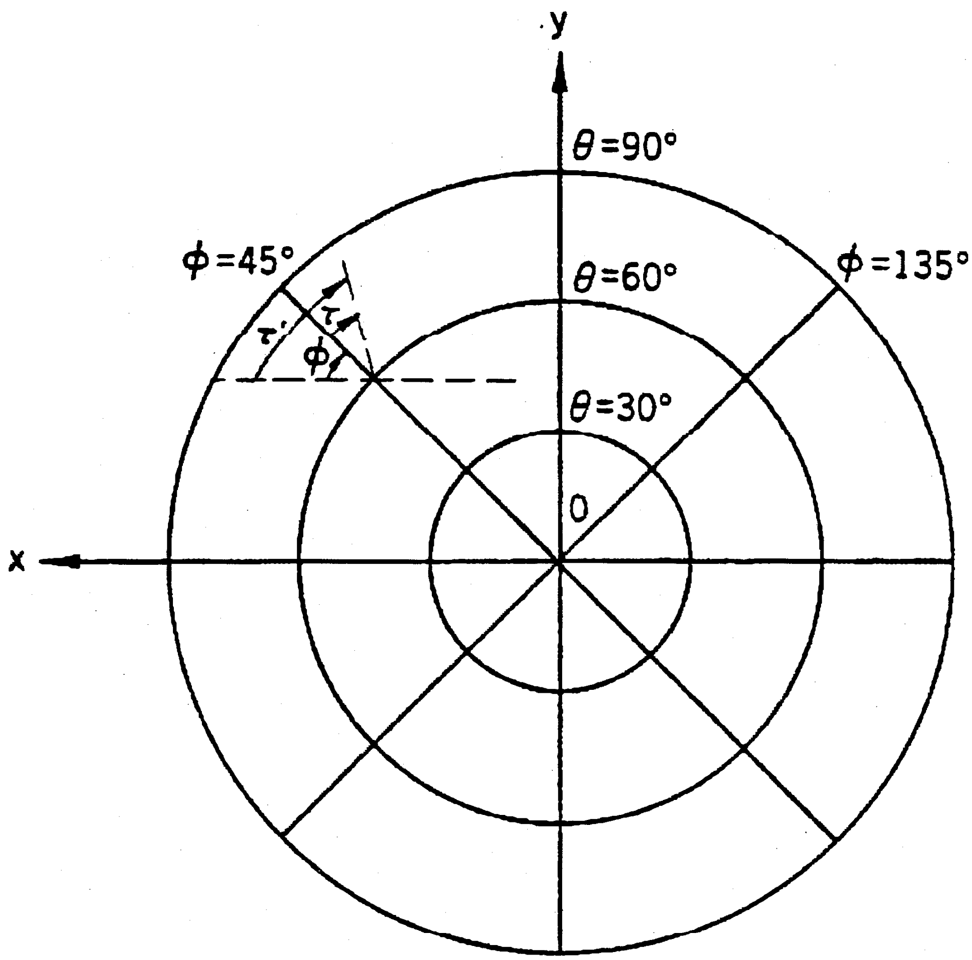


Figure 10. Schematic showing how the tilt angle, τ', in the modifiied θ-φ coordinates is related to the tilt angle, τ, of the θ-φ coordinate system.

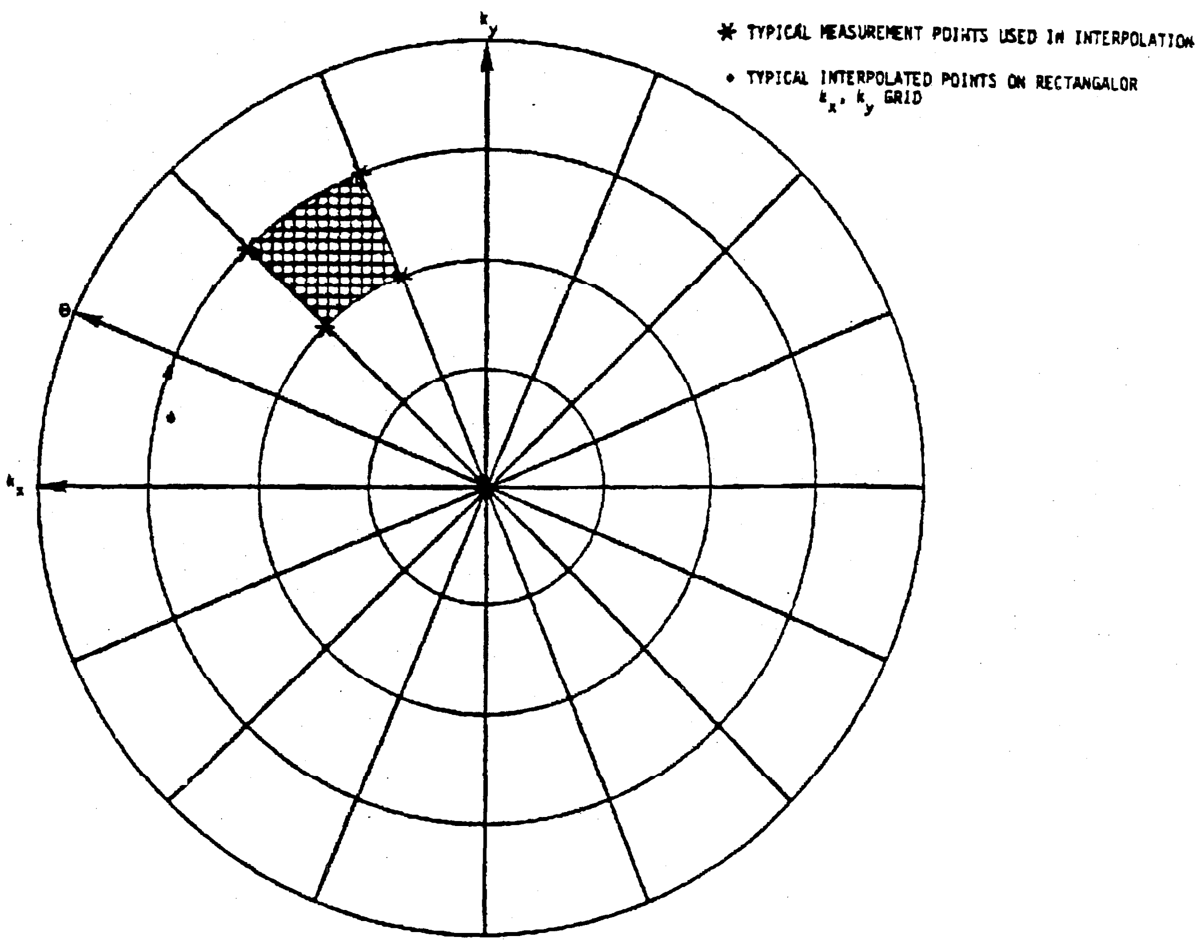


Figure 11. Schematic of interpolation from θ, φ measured grid to $k_x$, $k_y$ grid. θ and φ increments are shown much larger than those actually used. Typically $\Delta\theta = 2^{\circ}$, $\Delta\phi = 5^{\circ}$.